



# An Efficient Experimental Model to Estimate the Performance of the Raise Borer Drilling Machine Using Linear and Nonlinear Regression Approaches in the Azad Dam in Iran

Sirvan Moradi<sup>1</sup> · Ali Aalianvari<sup>1</sup> · Abbas Aghajani Bazzazi<sup>1</sup>

Received: 14 June 2023 / Accepted: 14 August 2023

© The Author(s), under exclusive licence to Springer Nature Switzerland AG 2023

## Abstract

This research evaluates the chief shaft in the Azad Dam hydroelectric power plant in Iran using a raise borer machine (RBM). Core samples were taken from the exploratory boreholes of the 210-m-long pressurized shaft. This study aims to determine new experimental models using linear and nonlinear regression approaches to estimate the operating parameters of RBM reaming, including daily progress rate, torque, thrust force, instantaneous penetration rate, power consumption, and the field's specific energy. Data on geological and operating parameters were sampled and recorded from two separate phases during field studies of the main shaft drilling. The results of field studies in secondary reaming, geological mapping, and laboratory results were used statistically. Statistical modeling showed that the rock quality index of RBM ( $Q_r$ ) has the highest correlation coefficient in linear relationships with the operating parameters. Rock quality designation (RQD) and  $Q_r$  are the most significant parameters affecting the RBM's rotational speed and torque estimate. Analyzing the development of nonlinear models showed that RQD performs well in estimating RBM's rotational speed and torque. Also, the field penetration index was a great measure to estimate the drilling's specific energy. The correlation coefficient in predicting the operating parameters of the RBM's penetration rate, rotational speed, and torque equaled 0.84, 0.71, and 0.7, respectively. Also, the RMSE value based on nonlinear regression for all three parameters equaled 0.24%, 1.35%, and 3.1%, respectively, indicating a low error in estimating RBM performance.

**Keywords** RBM's performance estimate · Penetration rate · Torque · Specific energy · Field penetration index · Rotational speed

## Introduction

Modern societies must dig the earth's crust for mining and construction activities. Human intervention in natural energy resources has expanded and encouraged societies to develop knowledge and technology with increasing energy needs. The RBM has been developed to fulfill the underground mining industry's needs and has found wide applications

in tunneling and infrastructure projects. Along with technological advancement, the need for drilling activities is also increasing. Mechanical drilling plays a significant role in this field and is an excellent alternative to blasting in mining and construction projects. RBM is a safe machine and provides shaft drilling between two levels of underground structures without using explosives. Mechanized drilling has many advantages, including a high drilling rate in favorable ground conditions, high safety and compatibility with the environment with minimum mixing in the ground. On the other hand, the high initial investment cost and complex ground conditions require performance estimate, design, and optimization (Bilgin et al. 2014).

Estimating the accurate RBM's operating parameters is one of the crucial evaluations in mechanized drilling. Field experience usually determines the context for the activity within a range. Shaterpour-Mamaghani et al. (2018) expressed that laboratory tests are expensive and

✉ Sirvan Moradi  
s.moradi@grad.kashanu.ac.ir

Ali Aalianvari  
ali\_aalianvari@kashanu.ac.ir

Abbas Aghajani Bazzazi  
a\_aghajani\_bazzazi@kashanu.ac.ir

<sup>1</sup> Department of Mining Engineering, Faculty of Engineering, University of Kashan, Kashan, Iran

time-consuming; therefore, determining optimum drilling techniques and parameters with minimum engineering effort and drilling experience is essential. Many researchers worldwide studied experimental and theoretical modeling to predict RBM's performance. The most significant of these studies are summarized in the following.

Hadjigeorgiou et al. (2009) described the problems of using an RBM for drilling in deep mines in South Africa. They presented a comprehensive approach to the interaction of stress structure on the stability of vertical or near-vertical excavations in underground excavation. Tumac and Balci (2015) proposed an experimental model for estimating normal and rolling forces on disc cutters and compared it with scientific tests and theoretical models. They concluded that although the rolling force predictions show some dispersion, it estimates the normal forces with high reliability. Also, Liu et al. (2015, 2016) evaluated rock hardness and confining pressure in predictive models. Their studies showed that increasing the confining stress restrains the extension of intermediate cracks, and the cutting efficiency is raised by increasing the distance between the cuts. Research by Zhi-qiang et al. (2015) showed that accurate geotechnical evaluation based on analysis in rock drilling, including crushing, rock cutting, wall stability, and hole deviation control, is one of the most significant rock mechanics problems in RBM drilling.

Shaterpour-Mamaghani et al. (2016) stated that the theoretical concept of shear penetration, RBM's performance, and other experimental models are evaluated using rock's mechanics properties obtained from exploratory drilling samples, geological surveys, and laboratory testing. The drilling risk in rock discontinuities using the RBM was reviewed by Shaterpour-Mamaghani et al. (2019). These researchers showed that besides the rocks' physical-mechanical properties, other factors, including mechanical and operating parameters, should be considered to evaluate the RBM's performance. Pan et al. (2019) proposed a model for predicting the performance of tunnel boring machines equipped with disk cutters. They generalized the experimental models based on rock properties, cutting geometry, and cutter shape to determine the drilling parameters, which is a simple and less expensive technique. Wang et al. (2020) studied the rock fracture prediction model in complex geological conditions. Using regression analysis, Shaterpour-Mamaghani and Copur (2021) developed experimental models to predict RBM's performance in vertical and inclined drilling based on rock properties.

From the studies mentioned above, it can be found that previous researchers have focused on using rock mechanics indices to estimate the RBM's performance and have not considered the field penetration index (FPI) and  $Q_r$ . This problem can be one of the compelling fundamental reasons for the inaccuracy in estimating experimental models with

the highest correlation. If the physical characteristics of the formation change, fundamental variations are made in the model and drilling rate relations, resulting in RBM's efficiency. The drilling parameters should be predicted before estimating the project's economic needs. Experimental approaches may encounter serious problems in fractured, weathered, and falling rock masses in shaft walls, stop drilling, and tool breakage; therefore, understanding the model of rock mass conditions around a shaft before and during drilling is essential (Hashiba et al. 2018).

This research calculates and records the geological logs' characteristics and the RBM's operating parameters during field studies with minimum error. The chief purpose of this study is to evaluate the experimental relationships of the RBM's operating parameters using the concepts of rock mechanics, physical petrography, and geological characteristics in the storage pump power plant of Azad Dam in Iran. Geological/geotechnical and rock mechanics parameters, including uniaxial compressive strength (UCS), RQD,  $Q_r$ , FPI, rock's internal friction angle (FC), rock mass adhesion strength, and rock mass rating (RMR), are the most significant factors directly affecting the success of shaft drilling (Shaterpour-Mamaghani et al. 2023). This research evaluates the effects of significant parameters that have yet to be given essential attention to improve the performance of the models and experimental relationships and to provide a new research field.

## Materials and methods

### Geology of the studied area

Azad dam and its transmission system are a part of the large water supply project in the west of Iran with an area of more than 220 thousand hectares. The main purpose of the Azad Dam construction is to supply agricultural, drinking, and industrial water. The dam is located in Kurdistan Province, with geographical coordinates of 34° 45' to 35° 46' northern latitude and 46° 05' to 48° 00' eastern longitude.

According to Iran's geological division, the dam is located northwest of the Sanandaj-Sirjan zone. In this zone, many metamorphic rocks are prominent outcrops in Esfandagheh-Hajiabad-Euclid-Abadeh-Isfahan-Golpaygan-Hamedan and Marivan. This zone has undergone significant phases of magmatism and metamorphism, especially the Laramide metamorphism, which is at the size of greenschist facies in the studied area until the Cenozoic. Therefore, it can be considered a metamorphic belt formed in the Late Triassic, the orogenic phase of the previous Simerian. Rocks that have been metamorphosed due to the Laramide event have a low intensity of metamorphism; therefore, schistosity

is not observed, and only slate faces and fractures have been developed.

The area's rocks are thin to medium-layered gray to dark gray sandstones, sometimes with phyllite, shale, and dark conglomerate sandstone interlayers. The oldest rocks of the studied area are dark gray and black clay shales that have been transformed into phyllite and slate due to regional metamorphism. From the upstream reservoir area to the downstream reservoir area of Azad Dam, the abundance of metamorphosed sandstone layers decreases, and phyllite and schist layers dominate. The grain sizes are medium to coarse, and the sandstone grains are predominantly siliceous. The joints and cracks of these layers are filled with carbonate, mainly calcite, with a thickness of about a few millimeters. Phyllite layers are rarely observed in the interlayers, whose thickness is at most several centimeters. Due to the difference in resistance with the sandstone layers, they are severely weathered and crushed. The color of these layers is light brown to gray. Figure 1 shows the geological situation of the studied area.

RBM is used for drilling shafts and other vertical structures in mining and civil engineering for the transportation system, ventilation, and hydroelectric power plant. Table 1 provides the RBM's specifications of Atlas Copco Robbins 73RHC, used in Azad Dam.

## Experimental studies

The Kurdistan Azad Reservoir Dam has been built on the Kumasi River, one of the significant tributaries of the Sirvan River in western Iran. Developing a deeper level and main shaft was necessary for drilling the dam's power plant. Also, the drilling and strengthening of shafts is undoubtedly the most challenging and expensive type of underground drilling. The main shaft, with a depth of 511 m, Fig. 2, was drilled using RBM. The samples were from the geological origin of igneous, metamorphic, and sedimentary rocks. The rock outcrop surface was tested to determine the samples' physical and mechanical properties, including UCS and elasticity modulus. According to the ASTM D455 Standard, the ratio of height to the smallest width of the sample equaled 2, and the large width to the small width equaled 1 (Heuze 1980). RQD values were obtained from the same boreholes where the representative samples were taken. Schmidt hammer tests were performed with an L-type Schmidt hammer on the NX Standard sample at twenty different points and repeated at least five times for each point (Çobanoğlu et al. 2008). The NX sample was prepared for the triaxial test with a ratio of diameter to height of 3:2 and device rigidity equaled 1 MN/mm by a coring machine manufactured by Farrance Wykeham, England, according to ASTM D2664 or ISRM-1983 Standard (Kovari et al. 1983).

## Drilling operation

In the Azad Dam, the RBM was installed at levels 1873 and 1640.9 m for drilling the main pilot shaft. At 1873 m, the RBM was placed in the working front of the upstream reservoir. A total of 133 drilling rods with a length of 1.52 m and a weight of 380 kg were used in shaft drilling. The pilot drilling diameter was 30 cm from the 1873 m level. After drilling to a depth of 7 m, signs of water leakage were observed; therefore, drilling to a depth of 16 m was done cautiously. Then, after drilling the pilot borehole and the reaming up operation, RBM was transferred to the next level located in the access tunnel, and the second phase of drilling was carried out. After preparing a special deviation meter device (GyrAB), it was found that the borehole has a deviation of 30 cm. In this period, a borehole with a depth of 75 m was drilled and injected to fix the water leakage. Then the pilot drilling was started again, which continued until the 30 cm pilot drilling was completed. The average progress rate was 3.34 m/day. After installing the reamer head with a diameter of 1.5 m, the pilot reaming operation started from the bottom to the top, and the average progress rate was 5.96 m/day. Figure 3 shows the position of the RBM and spindle during the reaming operation. Also, Fig. 4 shows the daily and cumulative progress rate in the shaft ream drilling.

## Results

### RBM's operating data

In this study, RBM drilling was done in sedimentary and metamorphic rocks and igneous dyke-shaped layers. The shaft's drilling depth and diameter were 550 and 1.5 m, respectively, starting in 2017 and completing in 2020. Operating parameters were recorded and calculated. The study was done on a series of exploratory borehole samples near the shaft. The total length of the boreholes was 560 m, and they were taken from different lithological units along the shaft.

The RBM's performance data were collected in two separate phases, and the rock mechanical tests were repeated four times for each sample except for the falling rock sample at levels 1743–1708. The  $Q_r$ , RQD, and RMR values were calculated in geological surveys and mapping. The UCS was carried out based on the techniques proposed by the International Society of Rock Mechanics (Hatheway 2009). The UCS test was conducted on milled core samples with length to diameter ratio of around 2.5 and a loading rate of 0.5 kN/s. The joint's dip and elasticity modulus were calculated according to laboratory tests. Also, experimental relationships during exploratory samples calculated the joint's FC and adhesion. The parameters of drilling depth, drilling time,

**Fig. 1** The location of the studied area on Iran's map and its geological map

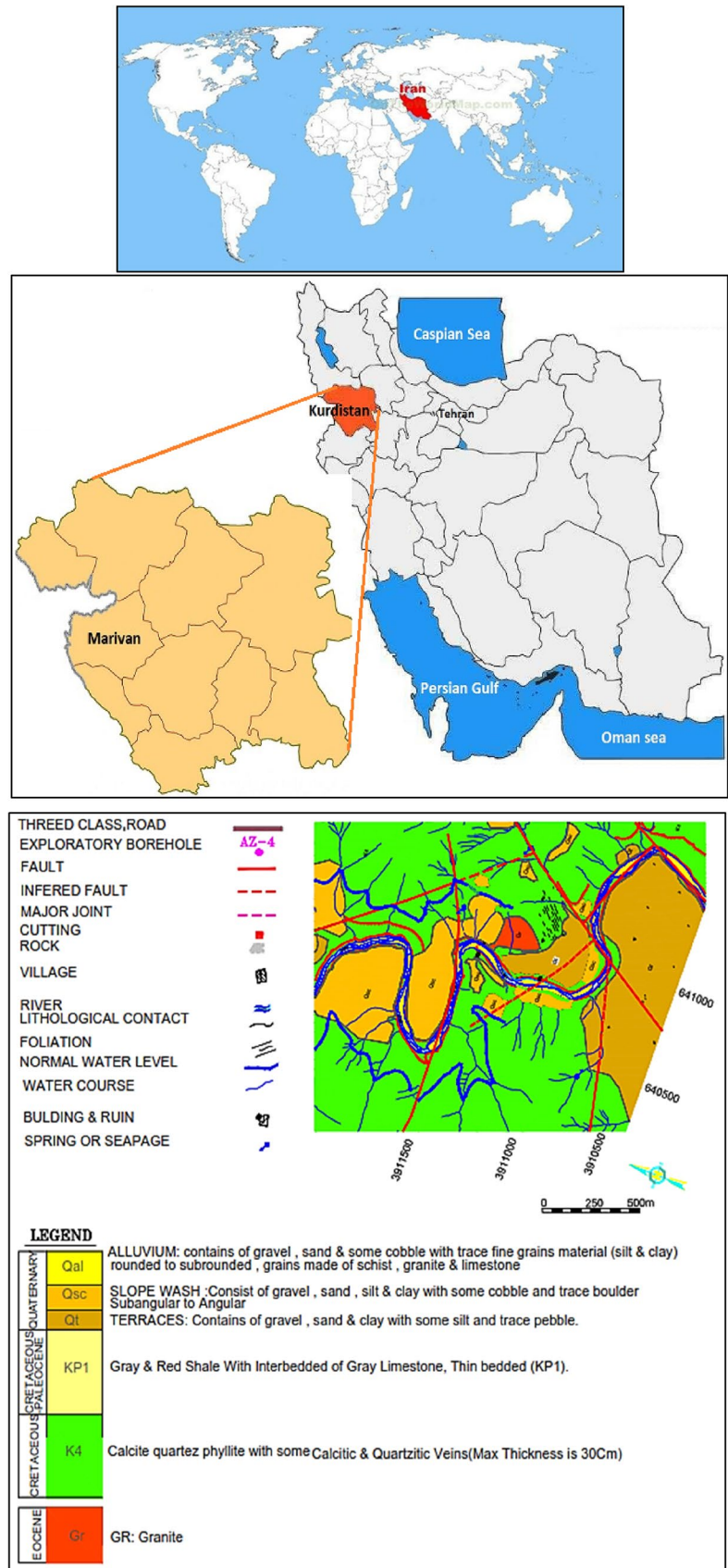




**Table 1** Main characteristics of 73RHC Raise Borer

Parameter	Value
Average drilling diameter	1.2 m
Average drilling depth	550 m
Torque	210 kNm
Thrust force	4159 kN
Power	200–250 kW
Maximum drilling depth	700 m
The rotational speed of the pilot hole	0–52 rpm
The rotational speed of reaming	0–17 rpm
Maximum drilling rate	7.1 m/min
Pilot diameter	254 mm
Reaming diameter	1524 mm

rotational speed (RPM), thrust force (F), and torque (Tq) were collected from the RBM's data. Instantaneous penetration rate (IPR), penetration per revolution of the drill head (P), net cutting rate (NCR), field's specific energy ( $SE_{\text{field}}$ ), power, and FPI were calculated as Eqs. (1–6), respectively.

$$\text{IPR} = \frac{L_e}{t_e} \times 60 \quad (1)$$

$$P = \frac{\text{IPR}}{\text{RPM}} \times \frac{1000}{60} \quad (2)$$

$$\text{NCR} = \text{IPR} \times A_{\text{sh}} \quad (3)$$

$$SE_{\text{field}} = \frac{\text{power}}{\text{NCR}} \quad (4)$$

$$\text{Power} = 2\pi \text{RPM} \cdot M_s \quad (5)$$

$$\text{FPI} = \frac{\frac{\text{Thrust cutter (kN)}}{\text{Penetration rate (mm/rev)}}}{\text{Penetration rate (mm/rev)}} \quad (6)$$

IPR is in m/h,  $L_e$  is the drilling length in meters,  $t_e$  is the drilling time in minutes, and NCR is in  $\text{m}^3/\text{h}$ . Also,  $A_{\text{sh}}$  is the cross-section area of the shaft, FPI is in  $\text{kN}/\text{mm}/\text{rev}$ , and P is in  $\text{mm}/\text{rev}$ . Power is the power of the rotary drilling machine in kW, RPM is the spindle speed in  $\text{rev}/\text{min}$ ,  $M_s$  is the spindle torque in kNm, and  $SE_{\text{field}}$  is the amount of energy required to break a rock unit in  $\text{J}/\text{m}^3$ .

The values of operating parameters, including RPM, Tq, F, IPR, P, power consumption, FPI, and  $SE_{\text{field}}$ , were calculated and presented in Table 2.

In most mechanized shaft drilling, there have limitations to geological mapping and rock mechanics laboratories; however, in this research, sections with reliable data were selected. Figure 5 shows the distribution curves of RBM's

geological and operating parameters recorded in the database. Based on the histograms, the range of data variations follows normal distribution functions.  $SE_{\text{field}}$ , FPI, and IPR's histograms show theoretically expected trends, and a slight deviation from statistical assumptions for other parameters can be ignored.

## Linear and nonlinear models

Simple regression analysis involves linear and nonlinear relationships between independent and dependent variables. It includes a regression variable X and a dependent variable Y. If two or more estimators are used for regression, each estimate may have a separate relationship with the input variable or may not identify the most significant independent variable. Therefore, it is a way to visually explain the pseudo-Venn diagram regression analysis concept (Cohen et al. 2013). In linear multivariate regression, the collective and individual participation of two or more independent variables ( $X_i$ ) in the variations of a dependent variable (Y) is expressed as Eq. (7).

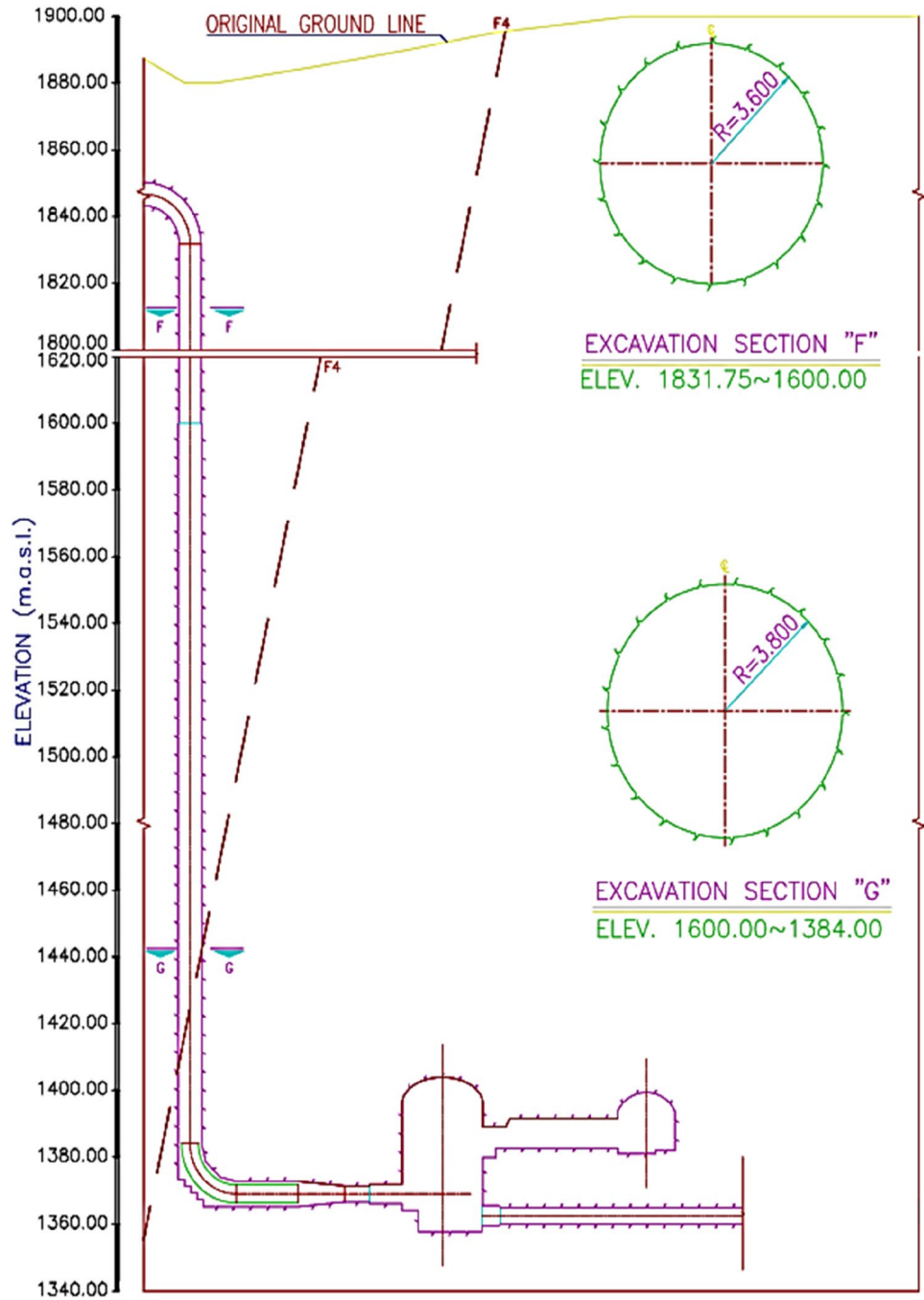
$$Y = a + b_1X_1 + b_2X_2 + \dots + b_nX_n \quad (7)$$

a is the intercept and  $b_1, b_2, \dots, b_n$  are the regression coefficients.

After collecting the data, this research used statistical analysis to find the relationships between the variable sets. Table 3 shows the correlation between RBM's operating parameters. Table 3 shows a strong correlation between parameters of UCS and  $SE_{\text{field}}$ , IPR and  $Q_r$ , Tq and  $Q_r$ , RPM and  $Q_r$ . Therefore, the RPM, Tq, IPR, and  $SE_{\text{field}}$  were chosen to determine the relationships with the physical–mechanical properties.

This research assumed that the relationship between the variables is linear using multiple linear regression, and the results are expressed as a normal distribution. The outputs were analyzed by SPSS software. Table 4 presents the statistical results of linear regression models. Also, the best results with the highest  $R^2$  values and the corresponding variance inflation factor (VIF) values are summarized in Table 4 based on Eqs. (8–11). The matrix's tolerance and VIF statistics or eigenvalues evaluate the multicollinearity intensity in ordinary least squares regression analysis. If the VIF is close to one, there is no collinearity between that X and the other quantities; however, if the VIFs > 1, there is collinearity between that X and the other quantities. If  $\text{VIF} > 5$ , the regression coefficient obtained for that term is inappropriate and that X is removed. Marquardt (1970) and Hair et al. (1995) suggested that a maximum VIF value of 10 is acceptable, while O'Brien (2007) stated that  $\text{VIF} > 5$  should be evaluated. Generally, a  $\text{VIF} > 10$  indicates the model has multicollinearity (Chatterjee et al. 2006). Hair et al. (2011) expressed that VIF should be

**Fig. 2** General view of the main shaft in Azad dam



less than 5 for each combined structure, which is the approved and accepted value by most researchers.

The best linear models for IPR, RPM,  $T_q$ , and  $SE_{field}$  are presented in Eqs. (8), (9), (10), and (11), respectively.

$$IPR = 0.04 + 0.436Q_r \quad R^2 = 0.68 \quad (8)$$

$$RPM = 1.52 + 1.95Q_r + 0.06UCS \quad R^2 = 0.61 \quad (9)$$

$$T_q = 30.69 + 31.77Q_r - 1.13E \quad R^2 = 0.51 \quad (10)$$

$$SE_{field} = 62.84 + 4.13Q_r - 46.3P \quad R^2 = 0.53 \quad (11)$$

Figure 5 shows the scatter plots of actual (measured) and estimated results of IPR, RPM,  $T_q$ , and  $SE_{field}$ . A relatively strong relationship was identified in the RBM's operating parameters, presented based on linear regression analysis and accepted as statistically significant (Fig. 6).

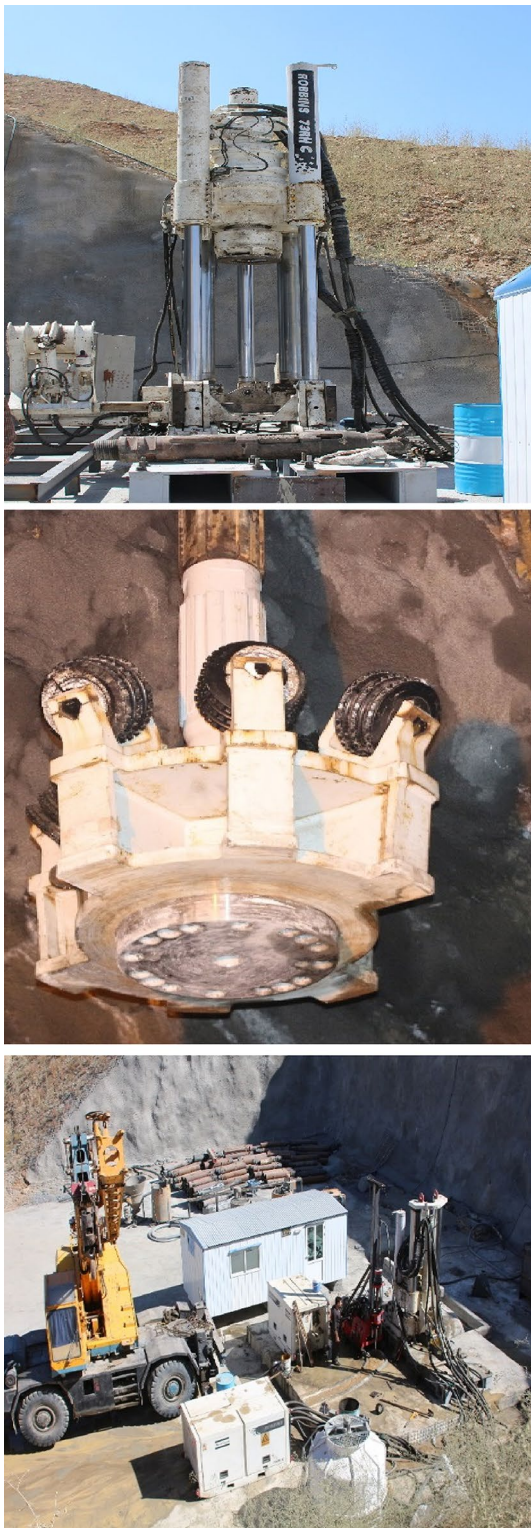


**Fig. 3** The position of the RBM and spindle at the bottom of the shaft during the reaming operation

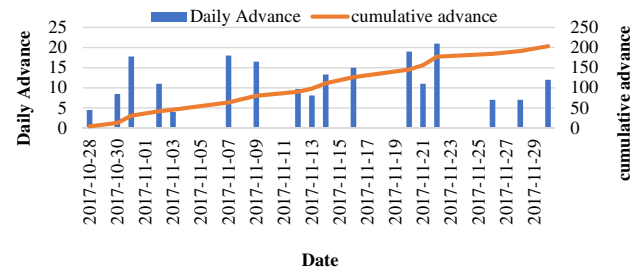


**Fig. 4** Daily and Cumulative progress rate in shaft ream drilling

Nonlinear regression analysis allows for examining the relative effect between independent and dependent variables. In this study, using multiple regression, the interaction analysis of the independent variable on other independent variables was considered based on the significant relationship. In linear and nonlinear multiple regression, collinearity between parameters was considered. For example, the correlation coefficient between  $Q_r$  and  $\phi$  equaled 0.94; however, due to the collinearity of the two parameters, they were not used in the equations.

The best-fitting nonlinear models between RBM's operating parameters, including IPR, RPM,  $T_q$ , and  $SE_{field}$ , are presented in Eqs. (12), (13), (14), and (15), respectively.

$$IPR = 0.127 + 0.011 \cdot UCS^{-0.13} + 0.984 \cdot C \quad R^2 = 0.84 \quad (12)$$

$$RPM = 9.54 + 7.07 \cdot \ln Q_r \quad R^2 = 0.71 \quad (13)$$

$$T_q = 14.49 + 0.279 \cdot RQD + 4.06 \cdot \ln(E) \quad R^2 = 0.7 \quad (14)$$

$$SE_{field} = 84.6 - 46.8 \times P + 0.39 FPI^{0.28} \quad R^2 = 0.66 \quad (15)$$

Detailed statistical results for the nonlinear regression models of the Eqs. (12–15) are summarized in Table 5. The p-value, t-value, and VIF values should be considered to obtain a reliable result. The t-value coefficient (equals the ratio of the estimated coefficient to the standard error value) and p-value (probability of the sample result obtained from the null hypothesis test) are created for each independent variable and show how a particular independent variable affects a dependent variable (Cohen et al. 2013). Therefore, the models obtained from linear and nonlinear regression analysis are statistically significant and reliable.

Figure 7 shows the comparison of estimated and measured results. A strong relationship is identified between operating parameters, accepted and analyzed as statistically significant based on nonlinear regression.

**Table 2** Measured/calculated operating parameters in reaming operation

Parameters	RPM (rev/min)	T <sub>q</sub> (kNm)	F (kN)	IPR (m/h)	P (mm/rev)	Power (kW)	FPI (kN/mm/rev)	SE <sub>field</sub> (kWh/m <sup>3</sup> )
Min	8	25	45	0.59	0.46	12.6	7.05	9.2
Mean	12.6	58.92	91.4	0.62	0.85	48.9	19.7	46.26
Max	16	97.5	120	1	1.58	102.6	53.11	86.2
Std	3.7	21.03	17.01	0.149	0.278	18.5	7.87	16.27

## Discussion

The rock samples tested in this research have different characteristics, from sedimentary rocks to hard igneous dykes, along with weak metamorphic rocks (phyllite and schist). Therefore, the number of points needs to be improved due to the wide variety. Considering shaft reaming from 1.5 to 8 m in diameter, it was possible to obtain accurate geological mapping and in situ rock mechanical tests; therefore, the data is accurate or close to reality. The normal distribution of parametric data is the most basic assumption of multivariate analysis. Considering the normality, the SE<sub>field</sub>, FPI, and IPR plots show theoretically expected trends. If the assumption is not fulfilled, the statistical tests are invalid and cannot be used (Dash et al. 2010).

The highest penetration and unit penetration rates were 1 m/h and 1.58 mm, respectively. Also, the lowest and highest RPM, T<sub>q</sub>, and SE<sub>field</sub> values have been provided in Table 1. Selecting the appropriate RBM is one of the significant factors in the economic success of drilling projects; therefore, the models proposed in this research should be used for initial approximation. Considering the linear cutting test of the cutting tools is close to the reality in estimating the RBM's performance; however, because of the sample size, the lack of experienced staff, and the high cost, it will be challenging to do it for the initial design and estimate. Therefore, the results should be strengthened by adding different capacities and diameters in the drilling to estimate the same RBM's performance.

The results of the nonlinear regression analysis of the study are consistent with the findings of Hughes's (1986) research, and considering some geological conditions and ignoring crushed and weathered regions, a good correlation can be expected. The proposed SE<sub>field</sub> models to approximate RBM's specifications considering FPI and IPR parameters agree with the research results of Delisio et al. (2014). Considering the direct relationship between SE and FPI and its inverse relationship with IPR, Eq. (15) is a reliable model and agrees with the results of Delisio et al. (2014).

Despite the outlier data, the regression model evaluation was highly accurate. The overall conformity of the model with the studied data was evaluated according to the error measurement criteria in Eqs. (16–19), which showed

the superiority of the nonlinear regression estimate model (Figs. 8, 9).

Model accuracy was evaluated based on statistical criteria, including correlation coefficient (R<sup>2</sup>), root mean square error (RMSE), standard error of prediction (SEP), and mean absolute percentage error (MAPE) that determines the accuracy of model fitness. The MAPE is the difference between the predicted and actual values of the model (Pearson et al. 2012; Neaupane and Adhikari 2006). The RMSE (Eq. 16) describes a measure of the best mean error in dependent prediction but does not provide any information about it. The MAPE (Eq. 17) measures precision in a series value fitted for statistical comparison.

$$RMSE = \sqrt{\frac{\sum_{i=1}^N (y_{pred,i} - y_{meas,i})^2}{n}} \tag{16}$$

$$MAPE = \frac{1}{N} \left[ \sum_{i=1}^N \left| \frac{(y_{pred,i} - y_{meas,i})}{y_{meas,i}} \right| \right] \tag{17}$$

y<sub>pred,i</sub> is the predicted value, y<sub>meas,i</sub> is the actual value, and n is the number of points that can be taken. The SEP is shown in Eq. (18). Bias (Eq. 19) represents the average value of the residual between the actual value and the prediction of individual errors, whether the model overestimates or underestimates the dependent variable (Palani et al. 2008).

$$SEP = \sqrt{\frac{\sum_{i=1}^N (y_{pred,i} - y_{meas,i} - Bias)}{n - 1}} \tag{18}$$

$$Bias = \frac{1}{n} \sum_{i=1}^N (y_{pred,i} - y_{meas,i}) \tag{19}$$

Figure 8 compares the basics of statistical tests of RMSE, MAPE, SEP, and R<sup>2</sup> statistical tests for regression models.

The absolute value of the prediction error for estimation models of RBM's operating parameters is shown in Fig. 9 based on its linearity or nonlinearity.

RMSE, R<sup>2</sup>, SEP, and MAPE are presented in Table 6 to examine the performance of the developed model and some existing prediction models. In most predictions, the error



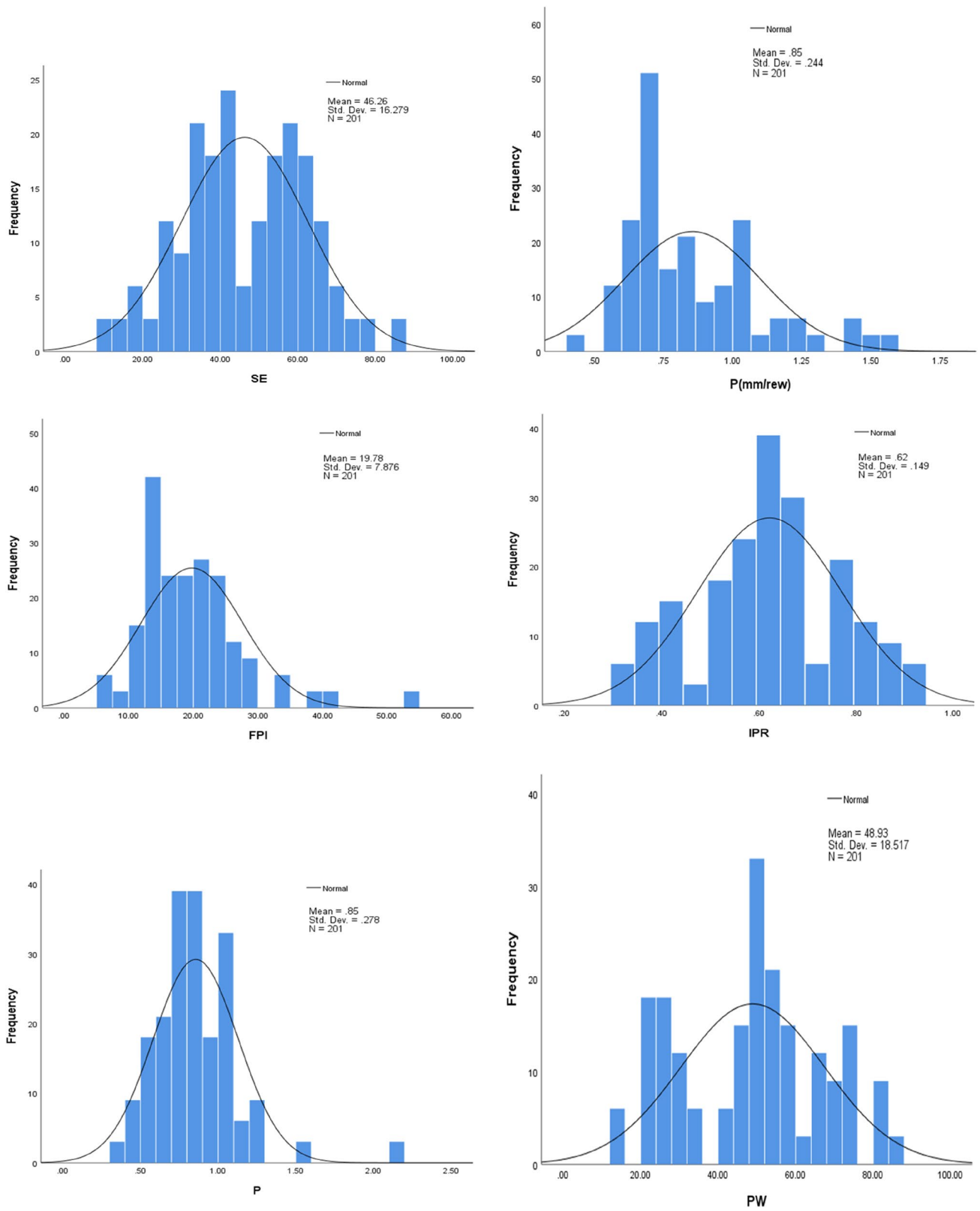


Fig. 5 Distribution curves and histograms of rock mass data and RBM's operating parameters

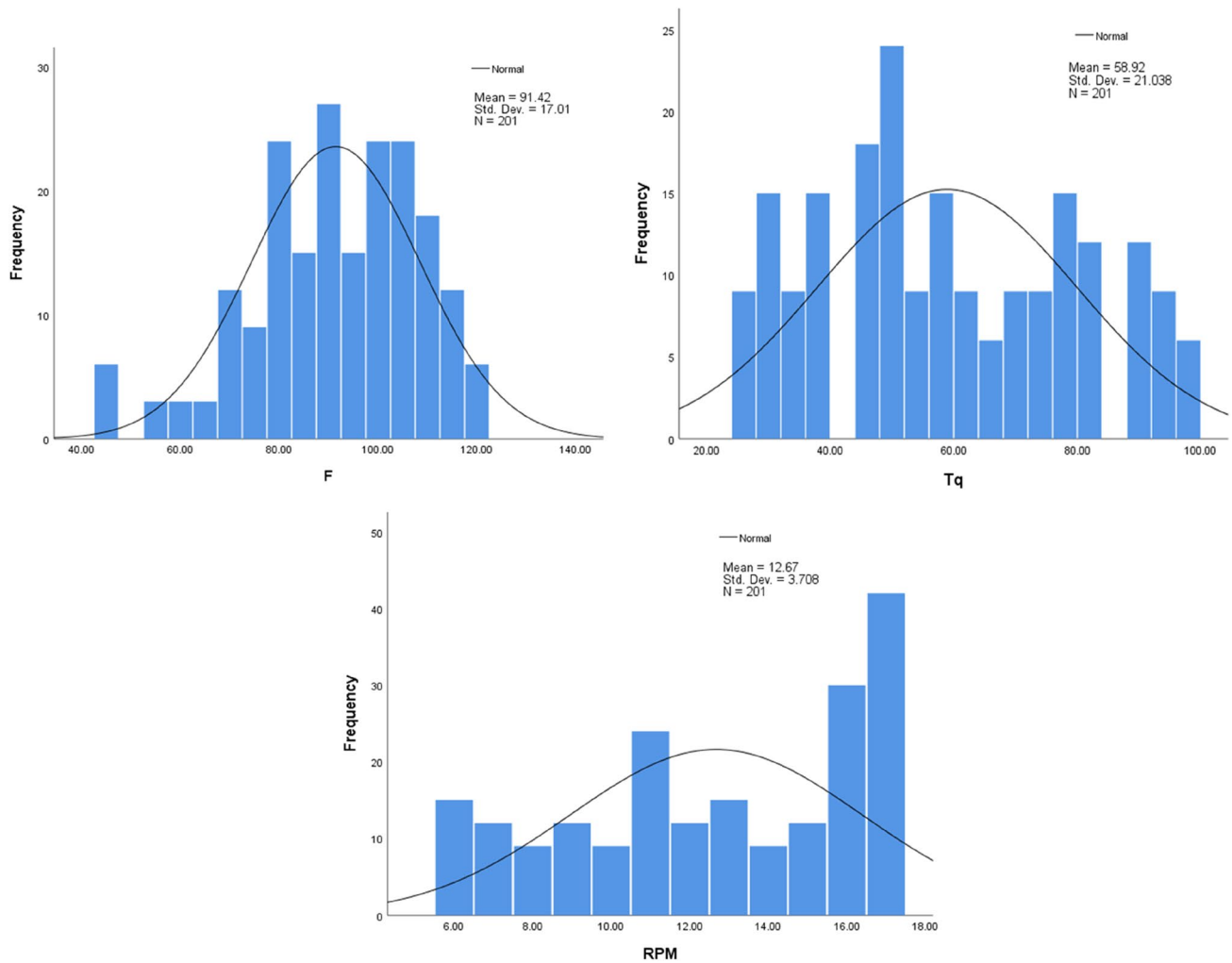


Fig. 5 (continued)

value of the estimated model based on nonlinear regression is smaller.

In Table 7, the statistical analysis is presented numerically according to the linear and nonlinear relationship of the model and geomechanical data.  $Q_r$  could estimate the RBM's operating parameters linearly, indicating the linear relationship between  $Q_r$  and the drilling performance. However, Barton (2000) believed  $Q_r$  is insufficient to estimate without adding rock-machine interaction parameters. According to Tables 4 and 5 and Fig. 8, the best matching of the estimated model with actual data is achieved using nonlinear relationships with the lowest error value and the highest accuracy.

## Conclusion

This research aimed to evaluate the effect of rock mass characteristics on RBM's performance to relate these parameters using statistical analysis. Regression analysis is one of the

most straightforward approaches to determining an experimental equation in RBM's operating parameters. The measured average  $T_q$  equaled 40.3 kNm, RPM equaled 13.4 rev/min,  $SE_{\text{field}}$  and measured IPR equaled 55.2 kWh/m<sup>3</sup> and 0.8 m/h, respectively. Linear regression analysis showed that the most significant parameter for estimating the performance of the IPR's drilling is  $Q_r$ ,  $Q_r$ , E, and UCS are the most significant parameters in estimating  $T_q$  and RPM. Nonlinear regression analysis showed that C and UCS are the most significant parameters in predicting IPR. The most significant influencing parameters in estimating RPM and  $T_q$  are RQD and  $Q_r$ .

According to regression analysis and based on field performance and laboratory data, the most significant estimator parameter in the models proposed in this research are UCS and RQD in the initial estimate of IPR and  $T_q$ . Also,  $Q_r$  can be used in the initial estimate of RPM. FPI and IPR can also be used to estimate the  $SE_{\text{field}}$ . RBM's operating parameters were evaluated according to regression models. IPR,

**Table 3** Correlation coefficients ( $R^2$ ) between the independent and dependent variables

	RQD	Qr	$\phi$	C (MPa)	RMR	E (GPa)	RPM (rev/min)	Tq (kNm)	UCS (MPa)	Log ( $\alpha$ )	F (kN)	IPR (m/h)	P (mm/rev)	PW (kW)	SE <sub>field</sub> (kWh/m <sup>3</sup> )
RQD	1														
Q <sub>r</sub>	-0.042	1	0.241												
$\phi$	0.027	0.941	1												
C (MPa)	0.111	0.017	0.089	1											
RMR	-0.003	0.141	0.365	0.208	1										
E (GPa)	-0.107	-0.238	-0.156	-0.073	-0.157	1									
RPM (rev/min)	0.155	0.501	0.524	0.704	0.403	-0.099	1								
Tq (kNm)	0.224	-0.486	0.224	0.011	0.226	-0.065	0.163	1							
UCS (MPa)	0.008	0.226	0.434	0.659	0.328	-0.017	0.473	-0.009	1						
Log ( $\alpha$ )	0.111	0.091	0.465	0.883	0.298	-0.104	0.602	0.131	0.739	1					
F (kN)	0.091	0.526	0.465	0.689	0.305	-0.109	0.613	0.011	0.757	0.96	1				
IPR (m/h)	-0.032	0.622	0.353	0.204	0.958	-0.132	0.387	0.222	0.333	0.294	0.306	1			
P (mm/rev)	-0.014	0.097	0.079	-0.127	-0.018	-0.202	-0.033	-0.028	0.001	-0.031	-0.013	0	1		
PW (kW)	0.012	0.208	0.519	-0.243	0.22	-0.031	0.145	-0.096	0.034	-0.053	0.017	0.145	0.037	1	
SE <sub>field</sub> (kWh/m <sup>3</sup> )	0.086	0.118	0.45	0.905	0.286	-0.117	0.807	0.019	0.778	0.963	0.988	0.292	-0.026	-0.03	1

C, cohesive strength of rock;  $\phi$  (°), friction angle of rocks; E, static elasticity modulus; PW, consumed reamer head power

**Table 4** Statistical results of linear regression models

Eq.	Regression Model	Independent variable	t-value	Sig	R <sup>2</sup>	Unstandardized coefficients B	Unstandardized coefficients std. error	Standardized coefficients beta	VIF		
8	Linear	Constant	2.12	0.038	0.68	0.118	0.056	0.832	1		
		Q <sub>r</sub>	12.02	0.000		0.832	0.032				
9	Linear	Constant	2.583	0.012	0.51	2.83	1.096	0.757	1.33		
		Q <sub>r</sub>	8.869	0.000		5.17	0.583			0.091	1.35
		UCS	1.062	0.092		0.022	0.021				
10	Linear	Constant	0.892	0.001	0.57	12.78	14.33	0.976	1.025		
		Q <sub>r</sub>	11.13	0.012		31.71	2.85			0.976	1.025
		E	-0.483	0.048		-1.13	2.35				
11	Linear	Constant	47.81	0.038	0.53	47.81	18.02	0.432	1.35		
		Q <sub>r</sub>	12.95	0.025						0.000	1.025
		P	-0.008	0.047							

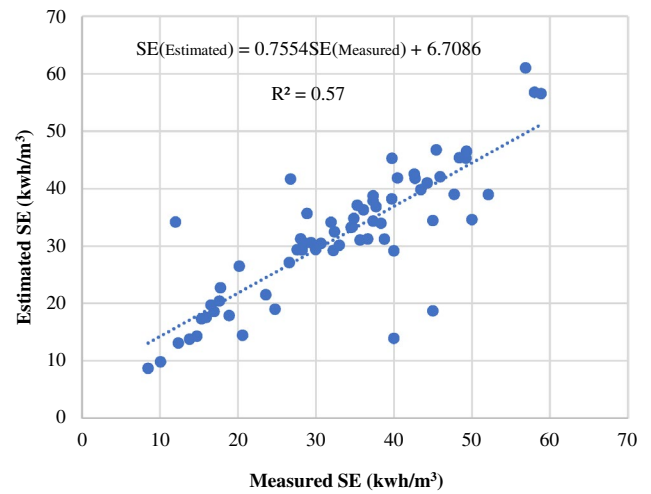
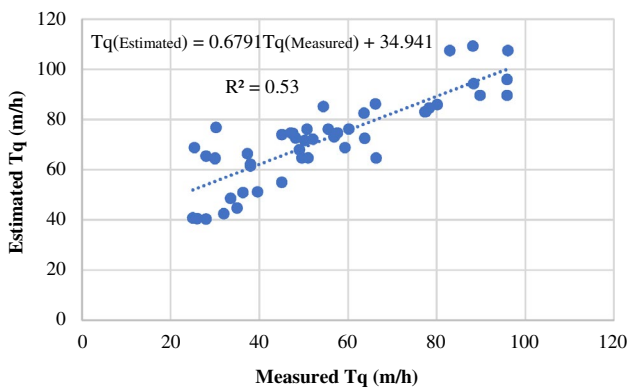
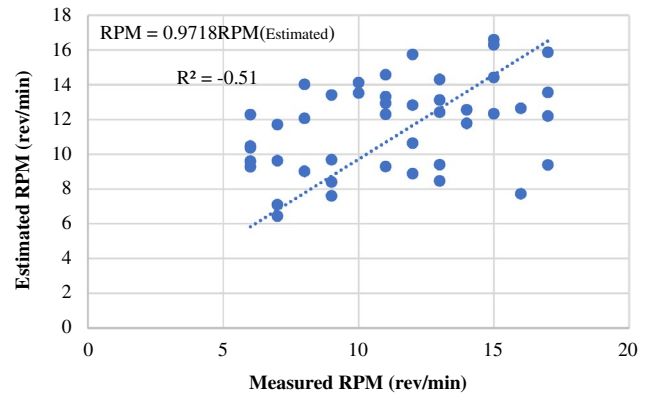
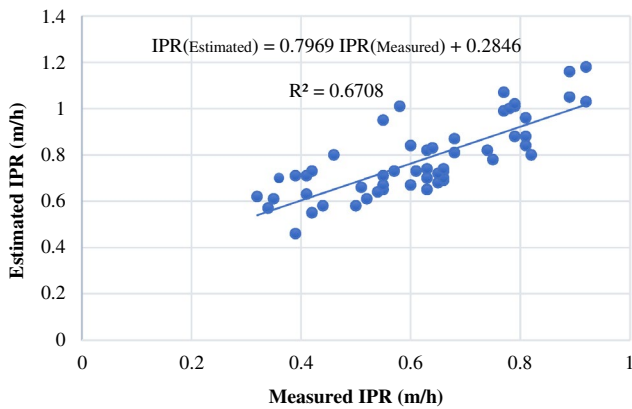


**Fig. 6** Scatter plots for measured and estimated operating parameters based on linear regression



**Table 5** Statistical results of nonlinear regression models

Eq	Regression model	Independent variable	p-value	T-value	R <sup>2</sup>	VIF	
12	Nonlinear	Constant	0.404	0.084	0.84	1.45	
		UCS	0	16.2			1.43
		C	0	4.73			
13	Nonlinear	Constant	0	9.42	0.71	1	
		Q <sub>r</sub>	0.014	2.52			
14	Nonlinear	Constant	0	4.79	0.75	1.120	
		RQD	0.046	0.74			1.021
		E	0.00	8.56			
15	Nonlinear	Constant	0	9.61	0.65	2.11	
		P	0.0	-7.62			2.11
		FPI	0.55	-0.006			

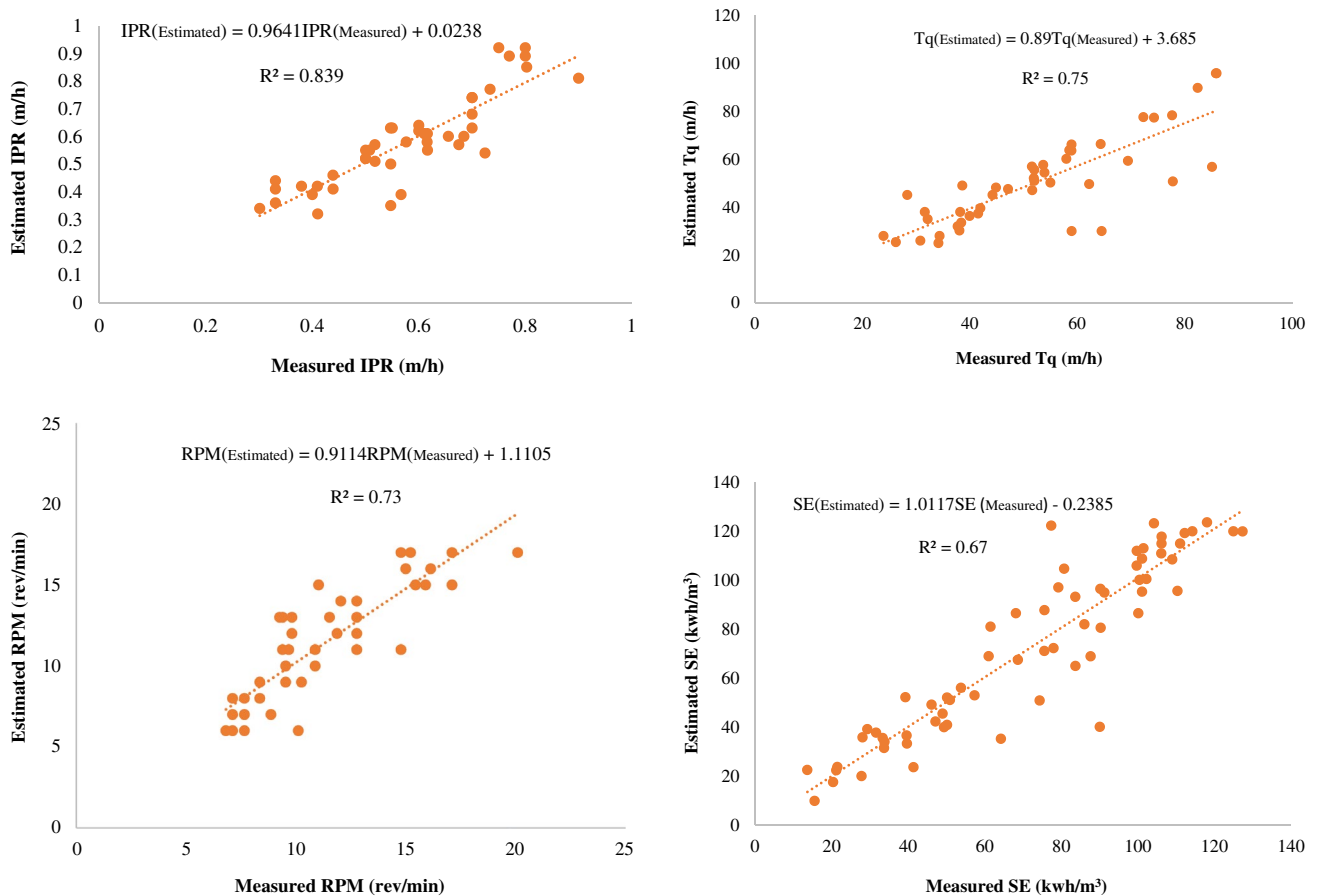


**Fig. 7** Scatter plots for measured and estimated operating parameters based on nonlinear regression

RPM and Tq’s correlation coefficient are 0.84, 0.71, and 0.7, respectively. RMSE values based on nonlinear regression for all three parameters equaled 0.24, 1.35, and 3.1%, respectively, indicating a low error in RBM’s performance estimate.

In this research, the geometry effect of the drilling bit is not considered. The comparison showed that the lowest

error with the highest prediction correlation corresponds to the nonlinear regression; however, according to the origin of rock formation, its error value is variable. Also, the error of the nonlinear regression model was the lowest in sedimentary and igneous rocks observed as dyke, and the highest in metamorphic rocks at a depth of 70–45 m and 167–135 m. The rock sample in this study showed a wide range of

**Fig. 8** Comparing the basics of statistical tests of RMSE, MAPE, SEP, and  $R^2$  for regression models

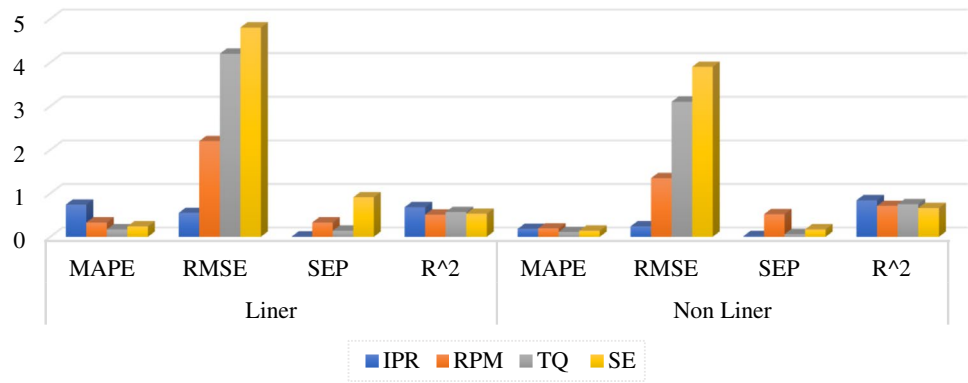


**Fig. 9** Comparing the error value of RBM's operating estimation models based on linear and nonlinear regression

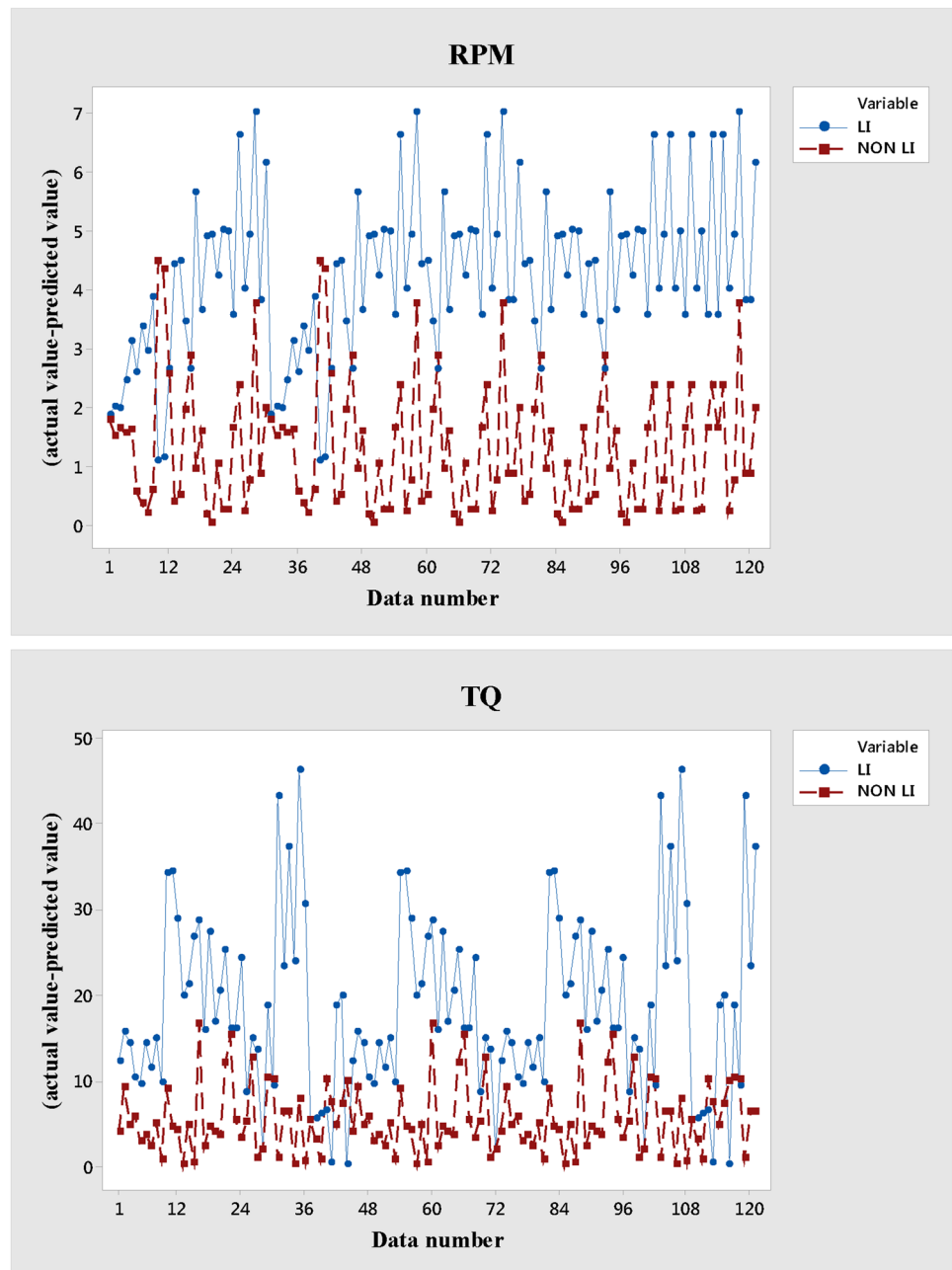
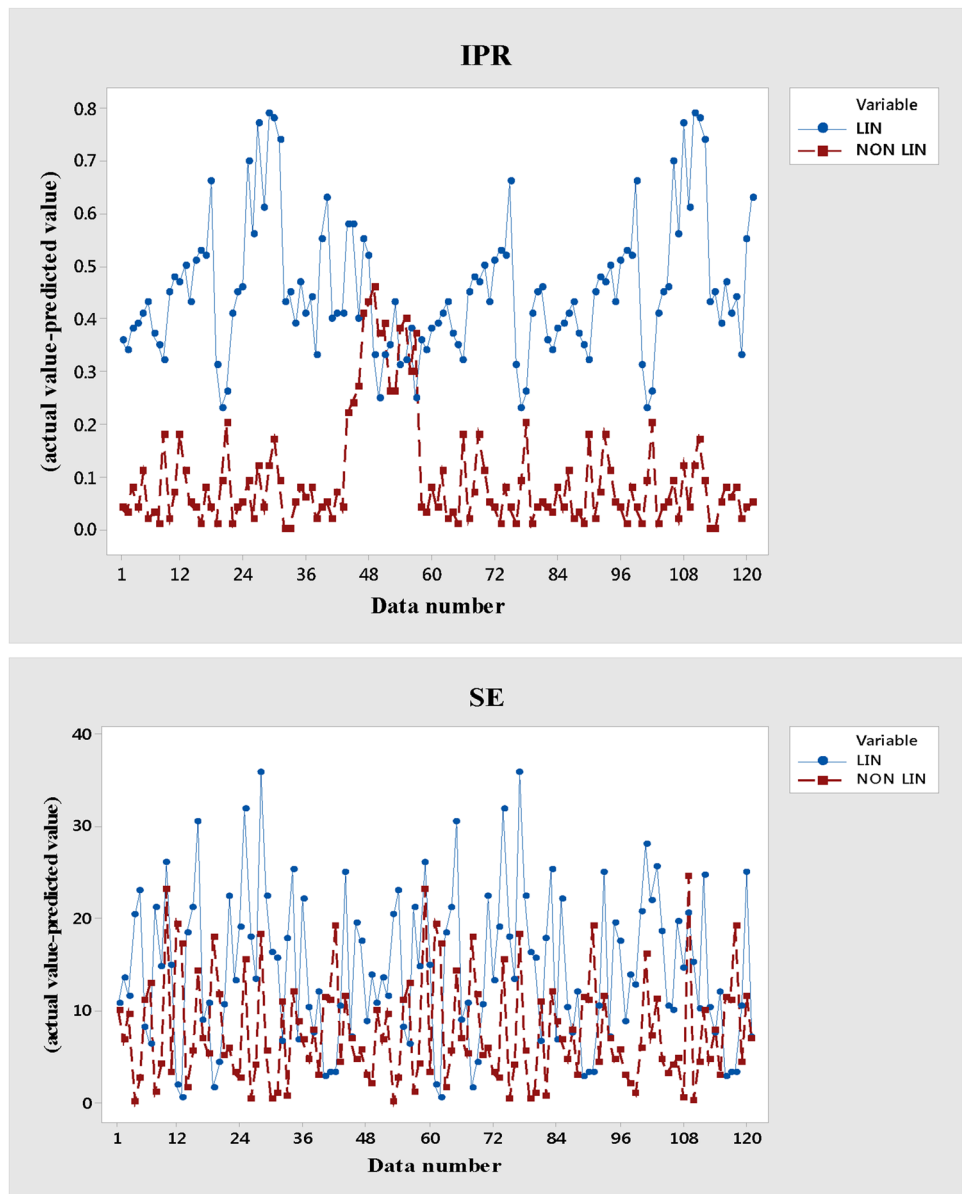


Fig. 9 (continued)



**Table 6** Comparison of different models for estimating the RBM's operating parameters based on statistical tests

Model	MAPE	RMSE	SEP	R <sup>2</sup>
<b>Linear</b>				
IPR	0.74	0.55	0.005	0.68
RPM	0.33	2.2	0.33	0.51
Tq	0.17	4.2	0.14	0.57
SE	0.24	4.8	0.91	0.53
<b>Nonlinear</b>				
IPR	0.18	0.24	0.015	0.84
RPM	0.19	1.35	0.52	0.71
Tq	0.11	3.1	0.06	0.75
SE	0.14	3.9	0.17	0.66

geological conditions; therefore, the proposed model can be used for different geological environments and RBMs with different capacities. This research can be done to develop more generalized performance prediction models by increasing the database and using different RBMs. Theoretical analyses in a full-scale laboratory are also needed to improve the model in the future.

**Acknowledgements** The authors express their sincere appreciation and gratitude to Dr. Shawgar Karami for her scientific cooperation. Also, we fully appreciate the editorial board of Modeling Earth Systems and Environment for their consideration. Hereto, we sincerely thank the anonymous reviewer for her/his professional review, in which her/his precious comments improved the scientific quality of the manuscript.

**Funding** The authors did not receive support from any organization for the submitted work.

**Table 7** Calculated operating parameters of the models in reaming

Parameters	Numeric value	Description	P (mm/rev)	Q <sub>r</sub>	RQD	C (MPa)	FPI (KN/mm/rev)	E (GPa)	UCS (MPa)	Equations (8–15)			SE (kWh/m <sup>3</sup> )
										IPR (m/h)	RPM (rev/min)	T <sub>q</sub> (kNm)	
1	0.6	Linear	0.6	1.7	66.4	0.6	19.9	6.0	53.3	0.8	8.1	78.4	40.5
2	1.3	Mean	1.3	2.7	100.0	1.3	53.1	7.7	75.0	1.2	11.3	107.8	14.7
3	0.2	Min	0.2	0.5	0.0	0.2	7.1	4.5	27.5	0.2	4.1	40.5	56.9
4	0.6	Max	0.6	1.7	66.4	0.6	19.9	6.0	53.3	0.8	13.4	40.3	55.2
5	1.3	Nonlinear	1.3	2.7	100.0	1.3	53.1	7.7	75.0	1.4	16.6	50.7	24.9
6	0.2	Mean	0.2	0.5	0.0	0.2	7.1	4.5	27.5	0.3	4.2	20.6	76.9

**Availability of data and material** The materials described in the manuscript, including all relevant raw data, will be freely available to any researcher wishing to use them for non-commercial purposes without breaching participant confidentiality.

**Code availability** Not applicable.

**Declarations**

**Conflict of interest** The corresponding author states no conflict of interest on behalf of all authors.

**Ethics approval** The manuscript has only been submitted to this journal at this time. The submitted work is original and has not been published elsewhere in any form or language, partially or fully. A single study has not been split into several parts to increase the number of submissions submitted to various journals or one journal over time. Results have been presented honestly without fabrication, falsification, or inappropriate data manipulation, including image-based manipulation. The authors have adhered to discipline-specific rules for acquiring, selecting, and processing data. No data, text, or theories by others have been presented as if they were the author’s own (‘plagiarism’). Proper acknowledgments of other works have been given.

**Consent to participate** All authors confirm their consent to participate.

**Consent for publication** All authors confirm their consent to publish the manuscript.

**References**

Barton NR (2000) TBM tunnelling in jointed and faulted rock. CRC Press, Rotterdam

Bilgin N, Copur H, Balci C (2014) Mechanical excavation in mining and civil industries. CRC Press, Boca Raton

Chatterjee S, Hadi AS, Price B (2006) Simple linear regression. Regression analysis by Example, pp 21–51

Çobanoğlu İ, Çelik SB (2008) Estimation of uniaxial compressive strength from point load strength, Schmidt hardness and P-wave velocity. Bull Eng Geol Environ 67:491–498. <https://doi.org/10.1007/s10064-008-0158-x>

Cohen J, Cohen P, West SG, Aiken LS (2013) Applied multiple regression/correlation analysis for the behavioral sciences. Routledge, England

Dash G, Paul J (2021) CB-SEM vs PLS-SEM methods for research in social sciences a technology forecasting. Technol Forecast Soc Change 173:121092. <https://doi.org/10.1016/j.techfore.2021.121092>

Delisio A, Zhao J (2014) A new model for TBM performance prediction in blocky rock conditions. Tunn Undergr Space Technol 43:440–452. <https://doi.org/10.1016/j.tust.2014.06.004>

Hadji Georgiou J, Esmaili K, Grenon M (2009) Stability analysis of vertical excavations in hard rock by integrating a fracture system into a PFC model. Tunn Undergr Space Technol 24:296–308. <https://doi.org/10.1016/j.tust.2008.10.002>

Hair JF, Anderson RE, Tatham RL, Black WC (1995) Multivariate data analysis, 3rd edn. Macmillan, New York

Hair JF, Ringle CM, Sarstedt M (2011) PLS-SEM: Indeed a silver bullet. J Mark Theory Pract 19:139–152. <https://doi.org/10.2753/MTP1069-6679190202>

Hashiba K, Fukui K, Kitahara M, Kiyama R, Okutsu K (2018) Estimation of rock mass conditions during shaft excavation with the raise



- boring method. In: ISRM international symposium-Asian Rock Mechanics Symposium. ISRM
- Hatheway AW (2009) The complete ISRM suggested methods for rock characterization, testing and monitoring. *Environ Eng Geosci* 15:47–48. <https://doi.org/10.2113/gseegeosci.15.1.47>
- Heuze FE (1980) Scale effects in the determination of rock mass strength and deformability. *Rock Mech* 12:167–192. <https://doi.org/10.1007/BF01251024>
- Hughes HM (1986) The relative cuttability of coal-measures stone. *Min Sci Technol* 3:95–109. [https://doi.org/10.1016/S0167-9031\(86\)90250-1](https://doi.org/10.1016/S0167-9031(86)90250-1)
- James G, Witten D, Hastie T, Tibshirani R (2013) An introduction to statistical learning. Springer, New York
- Kovari K, Tisa A, Einstein HH, Franklin JA (1983) Suggested methods for determining the strength of rock materials in triaxial compression: revised version. *Intl J of Rock Mech Mining Sci Geomechanic Abs* 20
- Liu J, Cao P (2016) Study on rock fracture with TBM cutter under different confining stresses. *Indian Geotech J* 46:104–114. <https://doi.org/10.1007/s40098-015-0148-4>
- Liu JS, Cao P, Liu J, Jiang Z (2015) Influence of confining stress on fracture characteristics and cutting efficiency of TBM cutters conducted on soft and hard rock. *J Cent South Univ* 22:1947–1955. <https://doi.org/10.1007/s11771-015-2714-4>
- Marquardt DW (1970) Generalized inverses, ridge regression, biased linear estimation, and nonlinear estimation. *Technometrics* 12:591–1256. <https://doi.org/10.1080/00401706.1970.10488699>
- Neaupane KM, Adhikari NR (2006) Prediction of tunneling-induced ground movement with the multi-layer perceptron. *Tunn Undergr Space Technol* 21:151–159. <https://doi.org/10.1016/j.tust.2005.07.001>
- O'Brien RM (2007) A caution regarding rules of thumb for variance inflation factors. *Qual Quant* 41:673–690. <https://doi.org/10.1007/s11135-006-9018-6>
- Palani S, Liong S-Y, Tkalic P (2008) An ANN application for water quality forecasting. *Mar Pollut Bull* 56:1586–1597. <https://doi.org/10.1016/j.marpolbul.2008.05.021>
- Pan Y, Liu Q, Peng X, Liu Q, Liu J, Huang X, Cui X, Cai T (2019) Full-scale linear cutting tests to propose some empirical formulas for TBM disc cutter performance prediction. *Rock Mech Rock Eng* 52:4763–4783. <https://doi.org/10.1007/s00603-019-01865-x>
- Pearson DW, Steele NC, Albrecht RF (2012) Artificial neural nets and genetic algorithms: proceedings of the international conference in Alès, France, 1995. Springer Science & Business Media, New York
- Shaterpour-Mamaghani A, Copur H (2021) Empirical performance prediction for raise boring machines based on rock properties, pilot hole drilling data and raise inclination. *Rock Mech Rock Eng* 54:1707–1730. <https://doi.org/10.1007/s00603-020-02355-1>
- Shaterpour-Mamaghani A, Bilgin N, Balci C, Avunduk E, Polat C (2016) Predicting performance of raise boring machines using empirical models. *Rock Mech Rock Eng* 49:3377–3385. <https://doi.org/10.1007/s00603-015-0900-1>
- Shaterpour-Mamaghani A, Copur H, Dogan E, Erdogan T (2018) Development of new empirical models for performance estimation of a raise boring machine. *Tunn Undergr Space Technol* 82:428–441. <https://doi.org/10.1016/j.tust.2018.08.056>
- Shaterpour-Mamaghani A, Copur H, Dogan E, Erdogan T (2019) Importance of physical-mechanical properties of rocks for application of a raise boring machine. *Tunnels and underground cities: engineering and innovation meet archaeology, architecture and art*. CRC Press, Florida, pp 1136–1143
- Shaterpour-Mamaghani A, Copur H, Balci C, Tumac D, Kocbay A, Dogan E, Altintas E, Erdogan T, Sirin O, Gumus A (2023) Suggestion of new models for predicting performance of raise boring machines based on indentation tests. *Tunn Undergr Space Technol* 138:105–181. <https://doi.org/10.1016/j.tust.2023.105181>
- Tumac D, Balci C (2015) Investigations into the cutting characteristics of CCS type disc cutters and the comparison between experimental, theoretical and empirical force estimations. *Tunn Undergr Space Technol* 45:84–98. <https://doi.org/10.1016/j.tust.2014.09.009>
- Wang J, Wang C, Han Z, Jiao Y, Zou J (2020) Study of hidden structure detection for tunnel surrounding rock with pulse reflection method. *Measurement* 159:107791. <https://doi.org/10.1016/j.measurement.2020.107791>
- Zhiqiang L, Yiping M (2015) Key technologies of drilling process with raise boring method. *J Rock Mech Geotech Eng* 7:385–394. <https://doi.org/10.1016/j.jrmge.2014.12.006>

**Publisher's Note** Springer Nature remains neutral with regard to jurisdictional claims in published maps and institutional affiliations.

Springer Nature or its licensor (e.g. a society or other partner) holds exclusive rights to this article under a publishing agreement with the author(s) or other rightsholder(s); author self-archiving of the accepted manuscript version of this article is solely governed by the terms of such publishing agreement and applicable law.